The Canadian Mineralogist
Vol. 41, pp. 905-919 (2003)

CHARACTERIZATION OF ARSENATE-FOR-SULFATE SUBSTITUTION IN SYNTHETIC JAROSITE USING X-RAY DIFFRACTION AND X-RAY ABSORPTION SPECTROSCOPY

DOGAN PAKTUNC[§] AND JOHN E. DUTRIZAC

CANMET, Mining and Mineral Sciences Laboratories, 555 Booth Street, Ottawa, Ontario K1A 0G1, Canada

ABSTRACT

Arsenic-bearing synthetic jarosite [$KFe_3(SO_4)_2(OH)_6$] was characterized to elucidate the form of the arsenic. The XANES spectra indicate that the As occurs exclusively as As^{5+}, nominally as AsO_4, consistent with the valence state of the arsenic in the reagents used for the syntheses. X-ray-diffraction analyses show that at least 9.9 wt.% AsO_4 can be structurally incorporated in the jarosite. Cell refinements show that both *a* and *c* increase slightly as the proportion of AsO_4 increases. The EXAFS spectra indicate that the As–O interatomic distances are uniform at 1.68 Å, and that the coordination numbers, 4.6 ± 1.7 to 5.4 ± 1.7, are indicative of tetrahedral coordination of the oxygen atoms around the central arsenic atom. The As–Fe interatomic distances are approximately 3.26 Å, with the coordination numbers being around 2, confirming that AsO_4 substitution for SO_4 occurs in synthetic jarosite. The larger arsenate ions seem to be accommodated in the tetrahedral sites by the expansion of the unit cell and by deficiencies in adjacent Fe–O(OH) octahedral sites. The observed increases in the unit-cell parameter *c* with increasing arsenate-for-sulfate substitution are similar to those of selenate and chromate substitutions for sulfate in jarosite. We believe that the Fe occupancy affects the amount of arsenate substitution, which is limited to about 17 mole % $AsO_4/(AsO_4 + SO_4)$. We contend that the charge imbalance caused by the substitution of arsenate is compensated by the partial protonation of the AsO_4 and SO_4, which would be consistent with the ionic species actually present in the synthesis media.

Keywords: jarosite, arsenic, arsenate-for-sulfate substitution, X-ray absorption spectroscopy, XAFS, EXAFS, XANES, replacement by selenate, replacement by chromate, charge balance.

SOMMAIRE

Nous avons caractérisé la jarosite [$KFe_3(SO_4)_2(OH)_6$] synthétique arsenifère afin d'élucider la forme de l'arsenic. Les spectres XANES indiquent que l'arsenic n'est présent que sous forme de As^{5+}, essentiellement AsO_4, et donc conformément à la valence présente dans les réactifs utilisés pour les synthèses. Les analyses par diffraction X montrent qu'au moins 9.9% de AsO_4 (proportion pondérale) peut être incorporé dans la structure. Des affinements de la maille élémentaire montrent que *a* et *c* augmentent à mesure que la proportion de AsO_4 augmente. D'après les spectres EXAFS, les distances interatomiques As–O sont uniformes et égales à 1.68 Å, et la coordinence, entre 4.6 ± 1.7 et 5.4 ± 1.7, concorde avec un agencement tétraédrique des atomes d'oxygène autour le l'atome central d'arsenic. Les distances interatomiques As–Fe seraient égales à environ 3.26 Å, avec une coordinence près de 2, ce qui confirme la substitution de AsO_4 au SO_4 dans la jarosite synthétique. Le groupe arsenate, plus volumineux, semble accommodé dans les sites tétraédriques par expansion de la maille et par lacunes dans les octaèdres Fe–O(OH). Les augmentations du paramètre *c* observées à mesure qu'augmente la proportion d'arsenate ressemblent à celles qui accompagnent la substitution du sélénate et du chromate au sulfate dans la jarosite. Nous croyons que la teneur en Fe affecte la portée de la substitution par l'arsenate, limitée à environ 17% [$AsO_4/(AsO_4 + SO_4)$, sur une base molaire]. Le déséquilibre des charges qu'implique la présence de l'arsenate serait compensé par la protonation partielle des groupes AsO_4 et SO_4, ce qui concorderait avec les espèces ioniques présentes dans le milieu de synthèse.

(Traduit par la Rédaction)

Mots-clés: jarosite, arsenic, substitution de l'arsenate au sulfate, spectroscopie d'absorption des rayons X, XAFS, EXAFS, XANES, remplacement par le sélénate, remplacement par le chromate, déséquilibre des charges.

§ *E-mail address:* dpaktunc@nrcan.gc.ca

INTRODUCTION

Jarosite-group minerals [$MFe_3(SO_4)_2(OH)_6$, where M is Na, K, Ag, Tl, H_3O, NH_4 and ½Pb] occur widely in nature, especially in the oxidized zone of sulfide ores (Dutrizac & Jambor 2000). Jarosite precipitation is also widely employed in the metallurgical industry to precipitate iron, sulfate and other impurities from processing solutions in a readily filterable form (Dutrizac 1983, Dutrizac & Jambor 2000). Arsenic, an undesirable element, is commonly present in processing solutions as arsenite (*i.e.*, As^{3+}) or arsenate (*i.e.*, As^{5+}) in various concentrations. Dutrizac & Jambor (1987) and Dutrizac *et al*. (1987) investigated the behavior of arsenic species during the precipitation of jarosite. Arsenate substitution limited to 2 wt.% AsO_4 was reported for synthetic natrojarosite [$NaFe_3(SO_4)_2(OH)_6$] crystallized at 150°C, and to 4 wt.% AsO_4 for synthetic jarosite [$KFe_3(SO_4)_2(OH)_6$]. Arsenate-for-sulfate substitution in jarosite-group minerals has also been reported, with up to 4.43 wt.% AsO_4 detected in jarosite from Laurium, Greece (Dutrizac *et al*. 1987). More extensive substitution is possible in other jarosite-group minerals, such as beudantite [$PbFe_6(SO_4,AsO_4)_4(OH)_{12}$], which has a variable AsO_4:SO_4 ratio and is accompanied by a low solubility of As in aqueous media (Dutrizac & Jambor 2000, Krause & Ettel 1989). The ability to incorporate arsenic, coupled with the relative stability of jarosite-type compounds and their disposal properties, makes jarosite-type compounds potentially attractive for the long-term disposal of arsenical wastes. Furthermore, synthetic jarosite–alunite [$KAl_3(SO_4)_2(OH)_6$] precipitates are also being considered for the immobilization of some products of radioactive fission and toxic metals (Hawthorne *et al*. 2000, Kolitsch & Pring 2001).

If jarosite-type precipitates are to be used for the control of arsenic, then it is important to understand how the arsenic is incorporated in the structure and whether the incorporation significantly destabilizes the jarosite. To provide some insight into these topics, we carried out a characterization study of synthetic jarosite precipitated in the presence of various concentrations of arsenic, added as dissolved potassium hydrogen arsenate. For characterization, we made use of X-ray diffraction, XANES spectroscopy and EXAFS spectroscopy.

EXPERIMENTAL METHODS

Synthesis of jarosite

The syntheses were carried out at 98°C using reagent-grade chemicals. One liter of 0.2 *M* $Fe(SO_4)_{1.5}$ – 0.3 *M* K_2SO_4 solution, at a pH of 1.40 and containing various concentrations of arsenic, was heated in a temperature-controlled 2-L reactor fitted with titanium baffles to improve the agitation of the solution. The pH of the solution was adjusted using H_2SO_4 or $MgCO_3$. Unpublished studies have shown that Mg does not form a jarosite-type compound; the Mg content of synthetic jarosite prepared from 0.5 M solutions containing Mg is <0.05% Mg. The arsenic was added as KH_2AsO_4, which contains only As^{5+}. Although acidic processing solutions are commonly considered to contain "arsenate", the redox potential – pH equilibrium diagram for the arsenic–H_2O system at 25°C (Pourbaix 1974) indicates that the simple arsenate species occurs only in strongly alkaline media. In the acidic environments characteristic of jarosite precipitation, the As^{5+} occurs almost entirely as the neutral H_3AsO_4 species and as $H_2AsO_4^-$. These species are important when the precipitation of As^{5+} from acid media is considered. Following the 24-h reaction period, the hot slurries were filtered. The precipitates were washed with at least 4 L of hot water and were subsequently dried in air for 24 h at 110°C. The solution concentrations and experimental conditions reflect the optimum range for jarosite precipitation (Dutrizac 1983, Dutrizac & Jambor 2000).

Characterization of the precipitates

All the dried precipitates were analyzed chemically for K, Fe, As and SO_4. The precipitates were dissolved in HCl, and the solutions were analyzed using atomic absorption spectroscopy (AA) or inductively coupled plasma – mass spectroscopy (ICP–MS). The accuracy for all the species is ±5%. All the precipitates were examined by Guinier–deWolff X-ray-diffraction analysis to confirm the presence of jarosite. The Guinier precision focusing camera sensitively records impurity phases, and we can demonstrate that as little as 0.25 wt.% scorodite ($FeAsO_4 \cdot 2H_2O$) in jarosite-type precipitates is detectable by this method. The samples were also examined using a Rigaku rotating anode X-ray powder diffractometer with Cu$K\alpha$ radiation, at a step scan of 0.04° and a scan rate of 4° per minute in 2θ. Refinements of the diffractometer data were carried out to determine the cell parameters, assuming a hexagonal cell with $a \approx 7$ Å and $c \approx 17$ Å. Jade, a commercial software package issued by Materials Data, Inc., was used for the cell refinements, where the fit parameters were a and c.

The XAFS experiments were carried out at the bending magnet beamline 2–3 and wiggler beamline 4–1 of the Stanford Synchrotron Radiation Laboratory. The samples were diluted with boron nitride to form a mixture containing about 1 wt.% As and were loaded into Teflon holders having 2.5 × 30 mm openings covered by Mylar windows. A silicon (220) double-crystal monochromator with 1 mm vertical slits was used for the collection of the EXAFS and high-resolution XANES spectra. The monochromator was detuned to 50% to eliminate harmonics. Arsenic foil was employed for energy calibration at the inflection point, 11867.0 eV. Nitrogen gas was used in the first and second ionization chambers, and argon gas in the third and fourth (fluorescence) detector. The samples were oriented at

45° with respect to the incident beam. The XAFS spectra were collected at room temperature in the fluorescence mode using a Lytle detector. The XANES spectra were obtained by scanning the monochromator at 0.2 eV steps over the edge region, and the EXAFS spectra, at 1.8 to 6.2 eV steps over the EXAFS region. The EXAFS analyses involved four scans of each sample and were averaged to increase the signal-to-noise ratio. The EXAFSPAK software (George & Pickering 1993) was used for data reduction, which included the standard procedures of background subtraction, per-atom-basis normalization with a victoreen polynomial, and extraction of the EXAFS by a cubic spline function anchored on the low-energy side at 11,885 eV. The curve-fitting program OPT in EXAFSPAK was employed for the EXAFS data analysis, using theoretical phase and amplitude functions generated in FEFF7 (Zabinsky *et al*. 1995) from scorodite by Foster (1999).

Results and Discussion

Chemical and mineralogical compositions

X-ray powder-diffraction analyses indicate that jarosite is the only phase in six of the samples containing up to 9.91 wt.% AsO_4 (Fig. 1, Table 1). There are

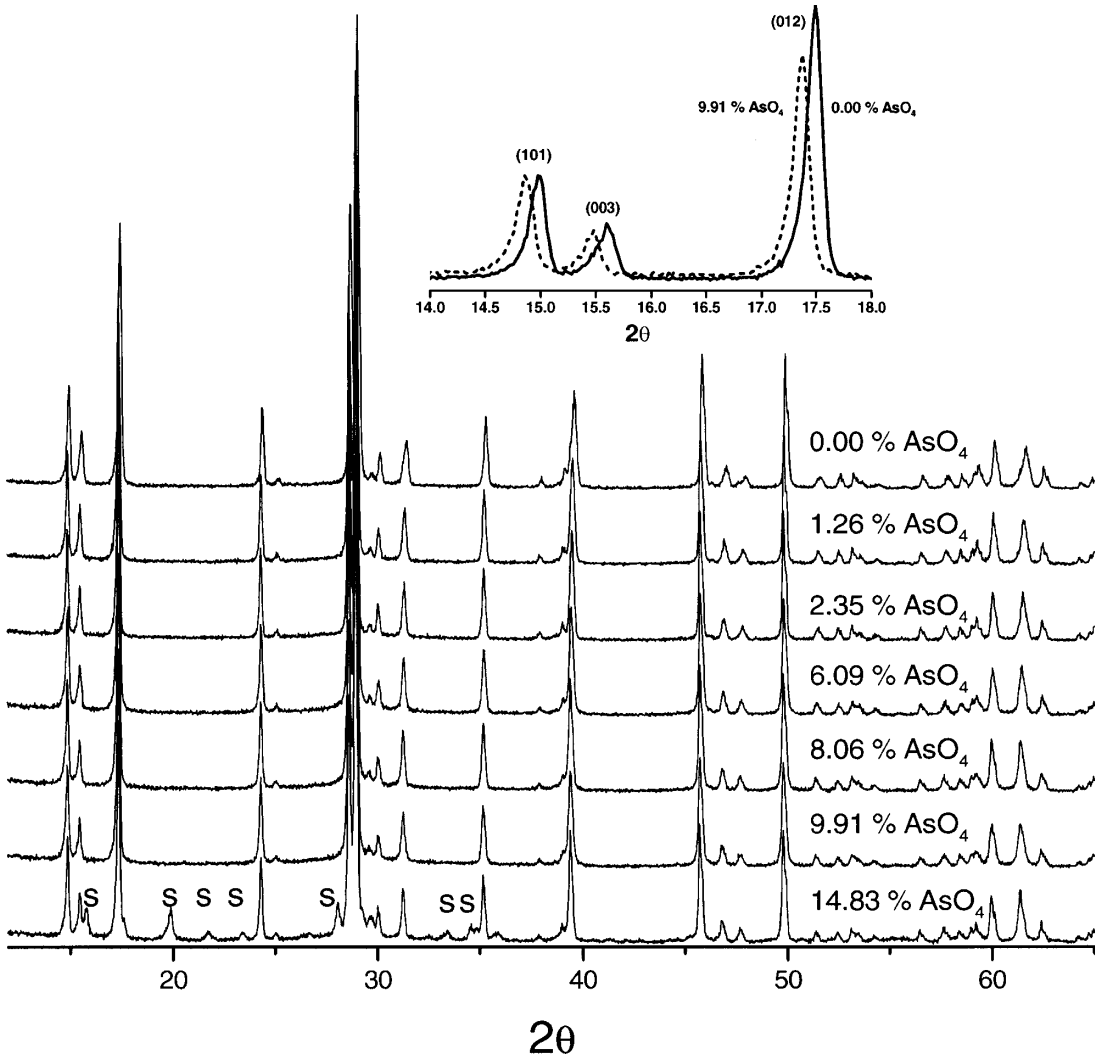

FIG. 1. X-ray powder-diffraction patterns of the jarosite precipitates. Numbers are AsO_4 concentrations in wt.%. Scorodite, occurring as a minor phase in the sample containing 14.83 wt.% AsO_4, is indicated by "s". The inset shows the displacement of the lines due to the substitution of 9.91 wt.% AsO_4 for sulfate.

no noticeable changes in the background to suggest the presence of an amorphous phase in the samples. The precipitate with 14.83 wt.% AsO_4 contains scorodite and jarosite. The amount of scorodite in this sample is 9.4 wt.%, on the basis of linear mixing involving the bulk chemical composition and the compositions of scorodite and synthetic jarosite (see Paktunc 1998). The composition of the jarosite is assumed to be similar to that of the precipitate with 9.91 wt.% AsO_4. The calculations show that scorodite is not possible in the other precipitates, confirming the XRD results and precluding the possibility of an X-ray-amorphous ferric arsenate. The results indicate that the maximum amount of AsO_4 that can be accommodated in the synthetic jarosite is between 9.9 and 14.8 wt.%. This is higher than the 4 wt.% AsO_4 reported for synthetic jarosite crystallized at 150°C (Dutrizac *et al.* 1987). At 150°C, efforts to synthesize jarosite from more concentrated arsenate-containing solutions resulted in the coprecipitation of scorodite, but this phase forms only from highly concentrated solutions at temperatures lower than 100°C. Dutrizac & Jambor (2000) reported AsO_4 concentrations in jarosite-group minerals of up to 4.5 wt.%, and Paktunc *et al.* (2003a) noted up to 5.4 wt.% AsO_4 in

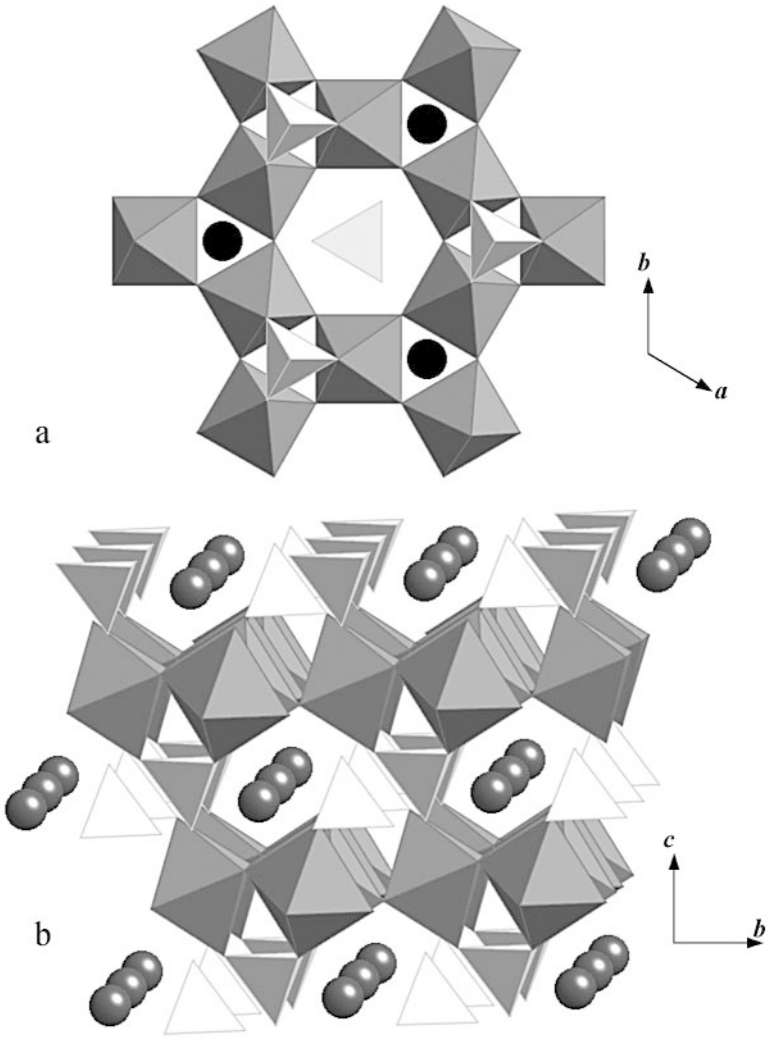

FIG. 2. Polyhedron representation of the jarosite structure as observed (a) on the (001) surface, illustrating the hexameric ring of corner-sharing Fe–O(OH) octahedra, and (b) an oblique view along the *a* axis. Large spheres represent the K ions.

jarosite-group minerals from the Ketza River (Yukon) ore and tailings.

The structural formulae of the synthetic jarosite precipitates calculated from the results of the bulk chemical analyses are also given in Table 1. The potassium is not adequate to fill the alkali sites in the structure. Furthermore, there is a deficiency in Fe of 0.50 to 0.54 moles, which means that the octahedral-site occupancy is approximately 83% (Table 1). Such deficiencies in Fe are not uncommon in jarosite-group minerals and compounds (Kubisz 1964, Alpers *et al.* 1989). Molar concentrations of sulfate decrease from 2.00 to 1.66 with increasing contents of arsenate. The maximum mole fraction of AsO_4 in the oxyanion site of the synthesized samples is 0.17, which means that for every mole of AsO_4, there are at least five moles of SO_4 in the structure. This is in accord with the findings of Dutrizac & Jambor (2000) in that there are no mineral compositions with AsO_4 mole fractions greater than about 0.25, and with Roca *et al.* (1999), who reported the presence of AsO_4 mole fractions up to 0.3 in jarosite in gossan ores.

According to Savage *et al.* (2003), synthetic jarosite can contain up to 30 wt.% As. Examination of their chemical data, however, suggests that the precipitates with As concentrations greater than about 8 wt.% appear to be mixtures rather than single-phase jarosite. There is not enough K in the reported compositions to qualify the precipitates as being jarosite alone. Synchrotron X-ray-diffraction analysis of the precipitates indicated the presence of an amorphous phase in the precipitates having As/(As + S) mole ratios of 0.11 and greater (Savage *et al.* 2003). This corresponds to our precipitates containing between 3.28 and 4.35 wt.% As (Table 1).

Crystal structure

The crystal structure of jarosite, based on the work of Kato & Miúra (1977), consists of sheets of Fe–O(OH) octahedra alternating with layers of sulfate tetrahedra and K ions in 12-fold coordination (Fig. 2). Each SO_4 tetrahedron shares three of its oxygen atoms with three Fe–O(OH) octahedra linked at the corners to form a ring-like structure. Sulfate tetrahedra on each side of the sheets of Fe–O(OH) octahedra are oriented either upward or downward, with three vertices having shared oxygen atoms with the Fe–O(OH) octahedra (Fig. 2). The S–O bond lengths are 1.545 Å for the basal oxygen atoms shared with the Fe–O(OH) octahedra and 1.468 Å for the apical oxygen atom.

There are gradual shifts in the peak positions with increased incorporation of arsenic. Linear fits to the variation of the *d* values as a function of AsO_4 indicate increases of 0.003 to 0.040 Å in *d* for variations of the AsO_4 mole fraction from 0 to 0.17. This forms additional supporting evidence for the substitution hypothesis describing the presence of AsO_4 in the precipitates, although we recognize that the cell parameters are also affected by variations in the occupancies of K and Fe.

Unit-cell parameters of the precipitates of synthetic jarosite were calculated by least-squares refinements from the powder-diffraction data. As shown on Figure 3, whereas *a* changes little with increasing arsenate substitution in the structure, *c* displays a more pronounced increase with increases in arsenate. The unit-cell parameter *a* is similar to the values reported by Dutrizac & Kaiman (1976) and Dutrizac & Jambor (1984) for synthetic jarosite, but is slightly greater than those for natural and synthetic jarosite reported by Brophy & Sheridan (1965), Menchetti & Sabelli (1976), and Kato & Miúra (1977). The *c* parameter of the As-free synthetic jarosite is slightly smaller than the previously published values for synthetic jarosite (Dutrizac & Kaiman 1976, Dutrizac & Jambor 1984). Natural jarosite has greater reported values for the *c* parameter. Dutrizac & Jambor (2000) pointed out that the variations in the *c* parameter are mainly due to substitutions at the alkali site. The unit-cell parameter *c* of hydronium jarosite is ~17.0 Å, and *c* of jarosite is ~17.1–17.3 Å. The alkali deficiencies, which are believed to be compensated by hydronium ions, vary from 0.10 to 0.12 (Ripmeester *et al.* 1986). Using the *c* parameter of 17.1 Å for jarosite, the indicated hydronium-for-potassium substitution would lower the *c* value to only 17.09 Å. In essence, hydronium-for-potassium substitution would have only a minimal effect on the *c* parameter in this case. Furthermore, there is no correlation between K and the *c* parameter; therefore, the observed variations in the *c* parameter of the jarosite precipitates do not seem to result from H_3O-for-K substitution.

TABLE 1. BULK CHEMICAL COMPOSITION AND FORMULA OF THE SAMPLES OF SYNTHETIC JAROSITE

	1	2	3	4	5	6	7
K wt.%	7.55	7.48	7.63	7.55	7.51	7.32	6.76
Fe	30.00	30.25	30.00	29.70	29.73	29.26	29.18
S	13.98	13.69	13.25	12.35	11.84	11.36	10.22
As	-	0.68	1.27	3.28	4.35	5.34	8.00
SO_4	41.88	41.02	39.70	37.00	35.47	34.03	30.62
AsO_4	-	1.26	2.35	6.09	8.06	9.91	14.83
K	0.89	0.88	0.91	0.90	0.90	0.88	
H_3O	0.11	0.12	0.09	0.10	0.10	0.12	
Fe	2.47	2.49	2.50	2.48	2.49	2.46	
SO_4	2.00	1.96	1.92	1.80	1.73	1.66	
AsO_4	-	0.04	0.08	0.20	0.27	0.34	
OH	5.44	5.27	5.47	5.29	5.20	5.27	
As/(As + S)	0.00	0.02	0.04	0.10	0.14	0.17	

The molar ratio As/(As + S) is equivalent to $AsO_4/(AsO_4 + SO_4)$. The elemental compositions of the bulk precipitates are given as reported; The coefficients of components of the jarosite formula are based on 2 (SO_4 + AsO_4). Samples 1 to 6 contain jarosite only, whereas sample 7 contains jarosite and scorodite.

Local structure

The positions of the absorption edges on the XANES spectra from five samples indicate that As occurs exclusively as As^{5+} in the jarosite precipitates (Fig. 4), and this observation is consistent with the valence state of the arsenic in the reagents used in the synthesis media. The k^3-weighted EXAFS spectra of the five precipitates of jarosite shown in Figure 5 are dominated by a sinusoidal wave resulting from the scattering of electrons between the central As and the first shell of O atoms. Fourier transformations of the k^3-weighted frequencies are shown on Figure 6. The major peaks at approximately 1.3 Å (uncorrected for phase shift) correspond to the As–O distance. The next prominent peaks, occurring at approximately 2.7 Å, correspond to scattering from the Fe atoms. These As–O and As–Fe peaks were isolated and back-transformed to k-space to form individual filtered EXAFS oscillations. Following this, the filtered spectra were fitted by non-linear least-squares methods to determine the coordination numbers, distances and Debye–Waller parameters by using the phase and amplitude functions derived from model compounds. The Debye–Waller parameter for As–Fe was fixed at 0.004 $Å^2$ for some samples following Paktunc *et al.* (2003b). Where this parameter was allowed to float, the resulting parameters were 0.003 $Å^2$. Because the two-shell fit resulted in slight shifts in the As–Fe peaks, a shell of multiple scattering was added to the EXAFS analysis following Foster (1999) and Paktunc *et al.* (2003a). Addition of the multiple-scattering shell improved the fit by correcting the displacements of the As–Fe peaks, as indicated in Figure 6.

The fit results, along with their uncertainties, are listed in Table 2. The As–O interatomic distances are uniform at 1.68 Å, and the coordination numbers range from 4.62 to 5.36. With the uncertainty value of ±1.7 estimated for the As–O coordination numbers, the above values suggest the tetrahedral coordination of oxygen atoms around the central As atoms. The As–Fe radial distances determined for the precipitates of arsenate-bearing synthetic jarosite are 3.25 and 3.26 Å. The corresponding coordination-numbers vary from 1.36 to 2.22. The lower end of this range was obtained by allowing the Debye–Waller parameter to float during the fitting analysis. The sample with scorodite and arsenate-bearing synthetic jarosite has a slightly longer As–Fe interatomic distance (*i.e.*, 3.33 Å), reflecting the contribution of the As–Fe distance in scorodite (*i.e.*, 3.36 Å).

In the jarosite structure, wherein an arsenate tetrahedron shares three of its oxygen atoms with three corner-linked Fe–O(OH) octahedra, interatomic distances between a S atom and the three nearest Fe atoms are

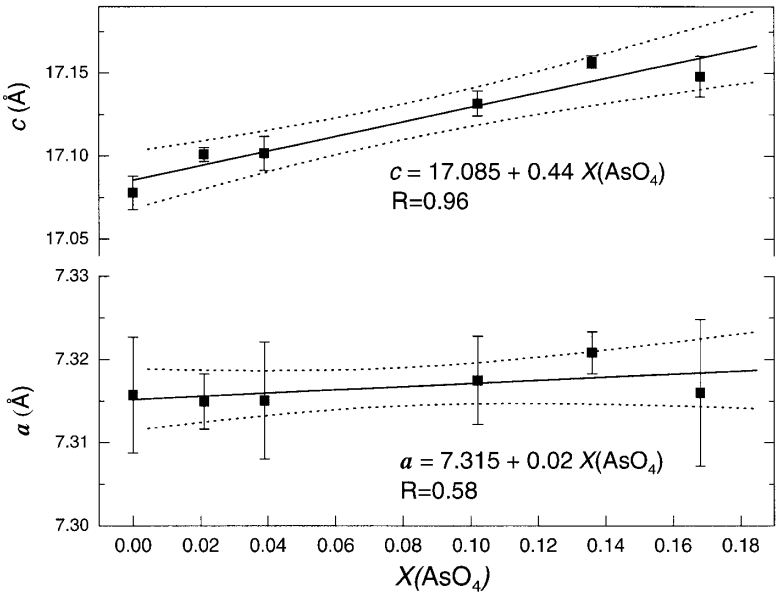

FIG. 3. Variation in the unit-cell parameters with mole fraction of arsenate [$X(AsO_4) = AsO_4/(AsO_4 + SO_4)$] in the synthetic jarosite precipitates. Error bars are three times the standard deviations. Dotted lines represent the 95% confidence bands of the linear fit. R is the correlation coefficient.

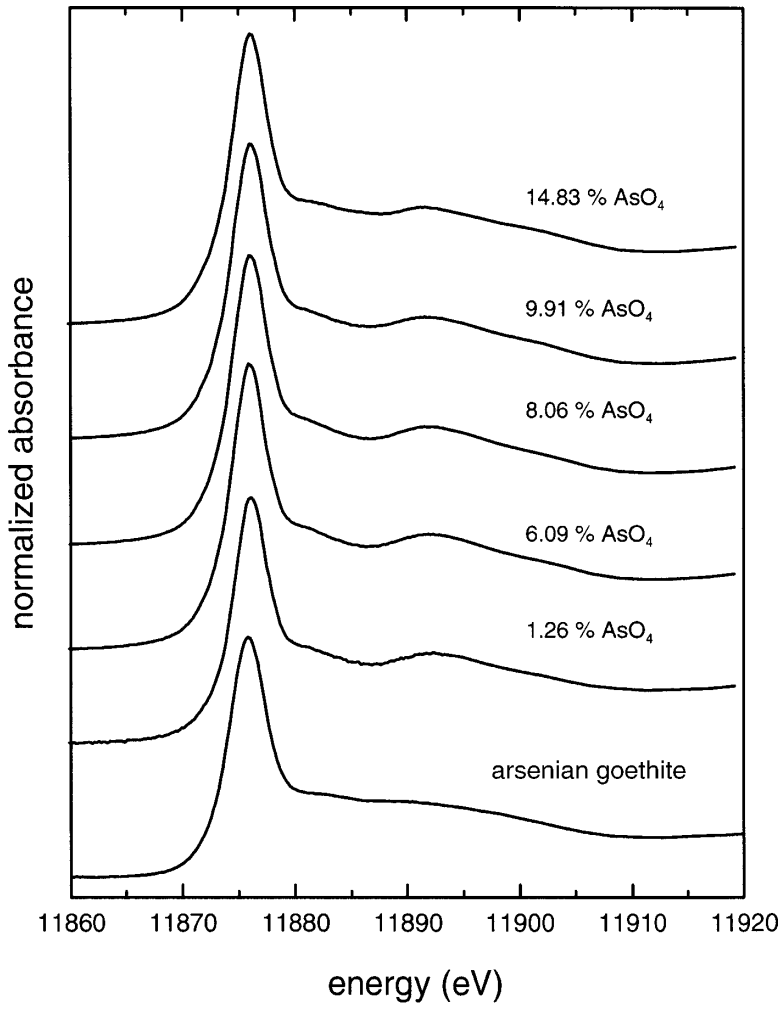

FIG. 4. As *K*-edge X-ray absorption near-edge structure (XANES) spectra of the synthetic jarosite precipitates having a range of arsenate concentrations. An As^{5+}-adsorbed goethite model is shown as a reference for the edge position.

3.23 Å on average. Considering the magnitude of the difference between the ionic sizes of arsenate and sulfate, the As–Fe distances, 3.25 and 3.26 Å, seem to be rather short, although they are not impossible to explain. The slightly lower coordination-numbers determined by EXAFS could be due to vacancies at the octahedral sites. The As–Fe radial distances are similar to those determined by EXAFS for a sample of natural jarosite (D. Paktunc, unpubl. data). Foster *et al.* (1998) reported an As–Fe distance of 3.25 Å in a bulk mine-waste, and interpreted this to possibly represent jarosite with arsenate substituted for sulfate. An As–Fe distance of 3.32 Å was reported by Savage *et al.* (2000) for jarosite in mine tailings from the Mother Lode gold district in California. The presence of As in the jarosite structure was interpreted by Savage *et al.* (2000) to be largely due to arsenate-for-sulfate substitution, although they did not exclude the possibility of limited adsorption by bridging two Fe–O(OH) octahedra. Among the As–Fe radial distances given by Savage *et al.* (in press) for a series of arsenate-containing precipitates, the sample of synthetic jarosite with trace amounts of an amorphous phase has an As–Fe distance of 3.27 Å, which is similar to our findings. These results further support the con-

clusion that jarosite is the only phase in the precipitates that contain less than 10 wt.% AsO_4. The possible presence of scorodite or an amorphous ferric arsenate is unfounded on the basis of the As–Fe interatomic distances of 3.36 and 3.37 Å for scorodite and amorphous ferric arsenate, as reported by Foster *et al.* (1998) and Paktunc *et al.* (2003b). The longer As–Fe distance, 3.33 Å, in the sample with 14.83 wt.% AsO_4 reflects the contribution of scorodite.

Szymański (1988) reported the bond lengths between the central As or S and the surrounding oxygen atoms in the beudantite structure to be 1.618, 1.618, 1.618 and 1.565 Å. These distances are too short in comparison with the As–O radial distance of 1.68 Å determined by EXAFS in this study and the range of distances from 1.66 to 1.70 Å based on EXAFS (Waychunas *et al.*1993, Fendorf *et al.* 1997, Foster *et al.* 1998, Randall *et al.* 2001, Paktunc *et al.* 2003a, b). The As–O interatomic distance is commonly 1.69 Å in bidentate–binuclear arsenate complexes in Fe oxyhydroxides, scorodite, arseniosiderite and other Ca–Fe arsenates.

Effect of arsenate-for-sulfate substitution on the structure

Two analogues of jarosite-type compounds, in which replacement of the sulfate is unlimited, are known.

TABLE 2. RESULTS OF EXAFS FITS SUMMARIZING THE LOCAL COORDINATION ENVIRONMENT AROUND A CENTRAL ATOM OF ARSENIC IN SYNTHETIC JAROSITE

No.	AsO_4	Shell	CN	R (Å)	σ^2 (Å^2)	E_0 (eV)
2	1.26	As–O	5.36 ± 0.33	1.68 ± 0.00	0.0019 ± 0.0004	–6.891
		As–MS	17.3 ± 7.53	3.11 ± 0.03	0*	**
		As–Fe	2.22 ± 0.34	3.25 ± 0.01	0.0040*	**
4	6.09	As–O	5.04 ± 0.20	1.68 ± 0.00	0.0021 ± 0.0003	–6
		As–MS	17.8 ± 4.45	3.09 ± 0.02	0*	**
		As–Fe	1.81 ± 0.21	3.26 ± 0.01	0.0040*	**
5	8.06	As–O	4.85 ± 0.16	1.68 ± 0.00	0.0019 ± 0.0002	–3.84
		As–MS	18.56 ± 3.90	3.08 ± 0.02	0*	**
		As–Fe	1.48 ± 0.39	3.26 ± 0.01	0.0028 ± 0.0014	**
6	9.91	As–O	4.88 ± 0.15	1.68 ± 0.00	0.0019 ± 0.0002	–4.35
		As–MS	18.53 ± 3.71	3.08 ± 0.01	0*	**
		As–Fe	1.36 ± 0.38	3.26 ± 0.01	0.0031 ± 0.0015	**
7	14.83	As–O	4.62 ± 0.16	1.68 ± 0.00	0.0017 ± 0.0002	–4.12
		As–MS	19.9 ± 3.30	3.09 ± 0.01	0*	**
		As–Fe	1.67 ± 0.16	3.33 ± 0.01	0.0040*	**

CN: coordination number, R: interatomic distance, σ^2: Debye–Waller parameter, E_0: energy offsct, * fixed value, ** value linked to the 1st shell E_0 value, MS: multiple scattering. Standard deviations represent uncertainties in the fits at the 95% confidence limit; uncertainties in the accuracy of the fits are ±1.7 for CN and ±0.01 Å for R of As–O, and ±0.4 for CN and ±0.02 Å for R of As–Fe, as determined by comparing the EXAFS analysis of a sample of scorodite to its nominal crystal-structure parameters. The amount of AsO_4 is expressed in wt.%.

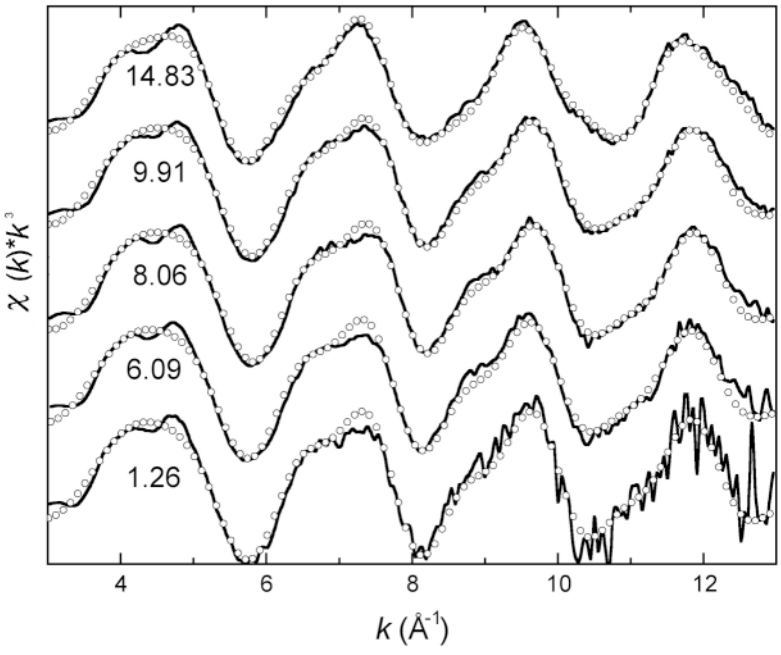

FIG. 5. k^3-weighted EXAFS spectra of the synthetic jarosite precipitates. Experimental spectra are shown by the solid lines, and the fitted spectra, by circles. Numbers indicate As concentrations as wt.% AsO_4.

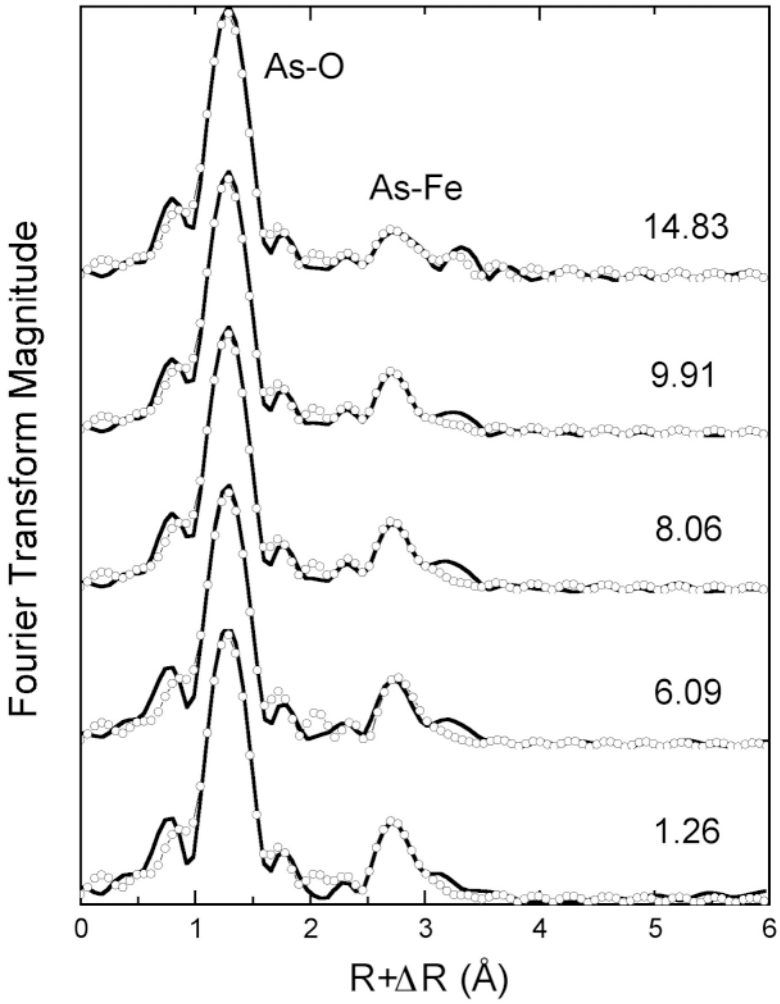

FIG. 6. Fourier-transformed EXAFS spectra. Transformation performed within the k interval of 3 to 13 Å at 0.01 Å intervals. Radial distances are not corrected for phase shift; experimental curves are indicated by solid lines, and the lines with circles are those of the fitted spectra. Numbers indicate As concentrations as wt.% AsO_4.

These are $NaFe_3(SO_4,SeO_4)_2(OH)_6$ (Dutrizac *et al*. 1981), wherein there is complete solid-solution between sulfate and selenate end-members, and $KFe_3(SO_4,CrO_4)_2(OH)_6$, wherein there is complete solid-solution between sulfate and chromate end-members (Baron & Palmer 2002, Dutrizac, unpubl. data). In both, the unit-cell parameters *a* and *c* gradually increase with an increase in the degree of substitution away from jarosite (Fig. 7). The following equations express these substitutions:

$c = 16.66 + 0.46\ X(SeO_4)$ R = 0.999 (calculated from Dutrizac *et al*. 1981)

$c = 17.11 + 0.37\ X(CrO_4)$ R = 0.980 (calculated from Baron & Palmer 2002)

$c = 17.17 + 0.30\ X(CrO_4)$ R = 0.976 (calculated from J.E. Dutrizac, unpubl. data)

$a = 7.32 + 0.07\ X(SeO_4)$ R = 0.996 (calculated from Dutrizac *et al*. 1981)

$a = 7.31 + 0.10\ X(CrO_4)$ R = 0.990 (calculated from Baron & Palmer 2002)

$a = 7.31 + 0.11\ X(CrO_4)$ R = 0.884 (calculated from J.E. Dutrizac, unpubl. data)

where a and c are the unit-cell parameters in Å, X is the mole fraction of SeO_4 and CrO_4, and R is the correlation coefficient. In the case of chromate-for-sulfate substitution, the expressions derived from two independent sources of data (Baron & Palmer 2002, Dutrizac, unpubl. data) are similar. The expressions for selenate-for-sulfate substitution also are similar, with the exception of the intercept value for c, which is lower because the alkali ion is Na instead of K. The slopes of the above expressions for c are approximately the same as that derived for the limited substitution of arsenate-for-sulfate (Fig. 3).

The expansion of the unit-cell parameter c caused by 100% substitution of selenate for sulfate is 0.46 Å, and that for chromate is 0.37 Å (calculated from Baron & Palmer 2002) and 0.30 Å (calculated from J.E. Dutrizac, unpubl. data). If 100% substitution of arsenate for sulfate were possible, the extrapolated expansion of the parameter c would be 0.44 Å. The parameter a expands by 0.1 Å for 100% substitution of chromate for sulfate and by 0.07 Å for 100% substitution of selenate for sulfate.

The S–O interatomic distances in tetrahedra are in the range of 1.43–1.50 Å for mineral structures (Hawthorne *et al.* 2000). Kato & Miúra (1977) noted that the S–O distances, which are 1.545 Å between the S atom and the basal oxygen atoms, and 1.468 Å between the S atom and the apical oxygen atom, are much longer than the typical S–O distances. On the basis of reported interatomic distances, the selenate and chromate ions are smaller than the arsenate ion, and all are larger than sulfate. Fendorf *et al.* (1997) and Peterson *et al.* (1997) reported the interatomic distances between Cr and O in tetrahedra to be 1.68 Å and 1.63–1.65 Å, respectively. The Se–O interatomic distances are 1.65 Å (Hayes *et al.* 1987) and 1.64 Å (Waychunas *et al.* 1995, Stoilova *et al.* 2003). Such similarities in the ionic sizes of chromate, selenate, and perhaps arsenate can explain the similar effects of their substitution on the unit-cell parameters of jarosite-type compounds.

There are three layers of tetrahedra composed of two tetrahedra in a unit cell. Each tetrahedron is positioned within the structure so that one of its basal planes is perpendicular to the c axis. Accordingly, any expansion due to replacement of the sulfate ions by larger chromate, selenate and arsenate ions would be directly re-

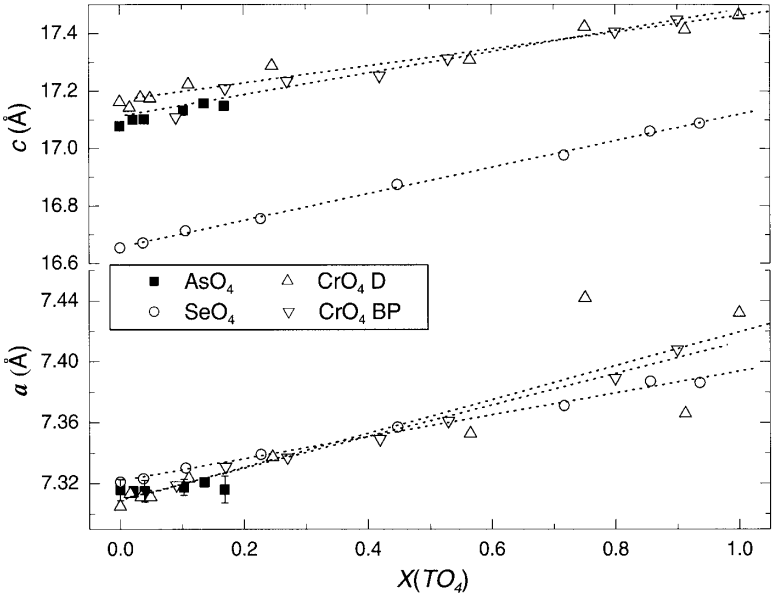

FIG. 7. Variation in the unit-cell parameters with substitution of sulfate by chromate and arsenate in synthetic jarosite, and by selenate in synthetic natrojarosite. $X(TO_4) = TO_4/(TO_4 + SO_4)$ where T represents As, Cr or Se. Dotted lines represent linear fits. CrO_4 D: J.E. Dutrizac, unpublished data; CrO_4 BP: data of Baron & Palmer (2002), with corrected values of c calculated from the data on unit-cell volume.

flected in the unit-cell parameters *a* and *c*. In one unit cell, 100% substitution corresponds to six tetrahedral sites. Extrapolation of the above expressions to the unit-cell scale indicates that substitution of one chromate tetrahedron for one sulfate tetrahedron results in the expansion of the unit-cell parameter *a* by 0.017 Å and *c* by 0.062 Å (Table 3). Corresponding values for one selenate tetrahedron substituting for one sulfate tetrahedron are 0.012 and 0.077 Å. Similarly, the unit-cell parameter *c* expands by 0.073 Å if one sulfate tetrahedron is replaced by arsenate.

For an independent assessment of the changes in the unit-cell parameters and their impact on the limit of substitution of sulfate ions, a digression into the crystal chemistry and geometry of the arsenate tetrahedron is necessary. The increase along the *c* axis, which results from the difference between the height of an arsenate tetrahedron and a sulfate tetrahedron, is 0.074 Å with the assumed parameters listed in Table 3. This increase is compatible with the above expansion of 0.073 Å determined from the unit-cell parameters (Table 3). Similarly, the increases along the *c* axis resulting from the differences between the heights of one selenate tetrahedron and one sulfate tetrahedron, and one chromate tetrahedron and one sulfate tetrahedron (*i.e.*, 0.077 and 0.064 Å, respectively) are comparable to the values determined from the unit-cell displacements resulting from the substitutions (*i.e.*, 0.077 and 0.062 Å).

The increases along the *a* and *b* axes, resulting from the differences in the O–O distances among the arsenate, chromate, selenate and sulfate tetrahedra, however, are greater than the displacements calculated for the unit-cell parameter *a*. These differences could be attributable to the short O–O distance assumed for the sulfate tetrahedron. This occurs because of the differences noted above between the unit-cell parameters of the natural and synthetic jarosites in that the sulfate tetrahedra of the synthetic compounds have greater O–O distances and shorter heights, which would result from wider O–S–O angles. Thus, a longer O–O distance, which is greater than the reported value of 2.53 Å for natural jarosite (Kato & Miúra 1977), would result in a smaller expansion of the parameter *a*. Alternatively, the O–O distances can be shortened by the distortion of the tetrahedron. Despite the similarities in the ionic sizes, the ionic radius of As^{5+} (*i.e.*, 0.335 Å) is greater than that of both Se^{6+} and Cr^{6+}. The ionic radius of Cr^{6+} in tetrahedral coordination is 0.26 Å and that of Se^{6+} is 0.28 Å (Shannon 1976). Both are twice as large as S^{6+}, but both still can fit into the tetrahedral interstice created by a close-packing arrangement of the oxygen atoms. Whereas the distortion of the selenate and chromate tetrahedra can accommodate the changes in the O–O distances, there is a limited accommodation of the arsenate tetrahedron because of the larger radius of the As^{5+} ion. If the O–O distance between the basal oxygen atoms of the arsenate tetrahedron is decreased to 2.72 Å, the height of the tetrahedron would become 2.26 Å. The difference in height between the distorted arsenate tetrahedron and the sulfate tetrahedron in the jarosite structure would then become 0.286 Å, which is almost twice as much as the displacement along the *c* axis and is not compatible with the increases in the unit cell based on empirical data (Table 3).

As discussed earlier, the observed occupancies of the octahedral site in the synthetic jarosite precipitates are about 83%. This value corresponds to about 1.6 Fe ion deficiencies in one unit cell. In other words, if one octahedral site is left unoccupied, the adjacent tetrahedral site sharing one of its basal oxygen atoms with the apical oxygen of the vacant octahedral site will have more space to accommodate the larger arsenate ion. Because there is only one octahedral site vacancy in one unit cell, the substitution of only one arsenate ion would be possible. This is the observed limit of arsenate substitution in a unit cell, and would help to better explain the Fe coordination numbers of 1.8 and 2.2, which are less than the nominal coordination number of 3 (Table 2, Fig. 8). In this configuration, we anticipate that the arsenate tetrahedron would slightly rotate toward the vacant site, with the two oxygen atoms shared with the Fe–O(OH) octahedra used as a hinge (Fig. 8). Furthermore, this vacancy hypothesis brings the As and Fe atoms closer, thereby making the As–Fe interatomic distances of 3.26 Å more realistic. Otherwise, the anticipated As–Fe

TABLE 3. COMPARISON OF THE DIFFERENCES IN UNIT-CELL PARAMETERS OF JAROSITE ARISING FROM THE SUBSTITUTION OF ONE SULFATE ION BY ARSENATE, CHROMATE OR SELENATE

	Cr	Se	As			S	
Based on XRD-derived unit-cell parameters (@ 16.7% substitution)							
c (Å)	17.174	16.733	17.158				
Δ*c* (Å)	**0.062**	**0.077**	**0.073**				
Based on crystal chemistry							
	(t)	(t)	(t)	(t)	(b)	(t)	(b)
X–O (Å)	1.65	1.67	1.70	1.70	1.71	1.55	1.55
X–O' (Å)	1.56	1.58	1.62	1.62	1.65	1.47	1.47
X–O* (Å)	*na*	*na*	*na*	*na*	1.66	*na*	*na*
O–*X*–O (°)	109.8	109.8	111.5	106.5	112.5	109.8	109.8
X–O (Å) average	1.62	1.64	1.68	1.68	1.68	1.53	1.53
O–O (Å)	2.69	2.72	2.81	2.72	2.82	2.53	2.53
T_h	2.102	2.128	2.122	2.260	2.121	1.975	1.975
ΔT_h ($T_h^X - T_h^S$)	0.128	0.153	0.148	0.286	0.147		
Δ*c* (Å) (one tetrahedron)	**0.064**	**0.077**	**0.074**	0.143	**0.073**		
Bond valence							
p(O)	2.08	2.08			1.83		2.08
p(O*)	*na*	*na*			1.33		*na*
p(O')	1.50	1.50			1.25		1.50

c: unit-cell parameter, Δ*c*: increase in the unit-cell parameter *c*; (*t*): based on tetrahedron parameters, (*b*): based on bond valence; *X*: S, As, Cr or Se; ΔT_h: difference in tetrahedron height with respect to sulfate, expressed in Å; *p*(O): sum of bond valences in valence units (v.u.); O*: basal oxygen dangling toward the vacant octahedral site necessary for arsenate incorporation; *na*: not applicable.

interatomic distances would have been around 3.35 Å, on the basis of theoretical considerations. In summary, the observed deficiencies in the octahedral sites seem to limit the incorporation of arsenic to one tetrahedral site in a unit cell or to about 18%. Naturally, another factor limiting the substitution of the arsenate ion is its greater charge relative to divalent sulfate, selenate and chromate. Therefore, the limited substitution likely reflects a combination of the size of the arsenate ion, the Fe deficiency and the charge of the resulting oxyanion.

In the arsenate tetrahedron, the basal atoms of oxygen receive bond valences from As, Fe and K atoms, whereas the bond valence of the apical oxygen (O') is limited to As bonding. The As–O and As–O' interatomic distances calculated by the bond valence concept and Baur's (1981) formalism of interatomic distances are 1.71 and 1.65 Å (Table 3). The distance between the As atom and the basal oxygen atom that is unconfined because of the proposed Fe vacancy in the octahedral site is 1.66 Å. In comparison to the values based on considerations of tetrahedron geometry, the longer As–O' distance (*i.e.*, 0.65 *versus* 0.62 Å), which would result in a higher displacement along the *c* axis, is compensated by a 1° increase in the O–*X*–O angle. This slight increase in the O–*X*–O angle is reasonable because the O–O' edges are shared with K–O polyhedra; thus, they are expected to be shorter on the basis of Pauling's (1929) second rule. The corresponding increase in the unit-cell parameter *c* is 0.073 Å, which is identical to the displacement along the *c* axis due to 17 mole% AsO_4 substitution for SO_4, as determined by XRD.

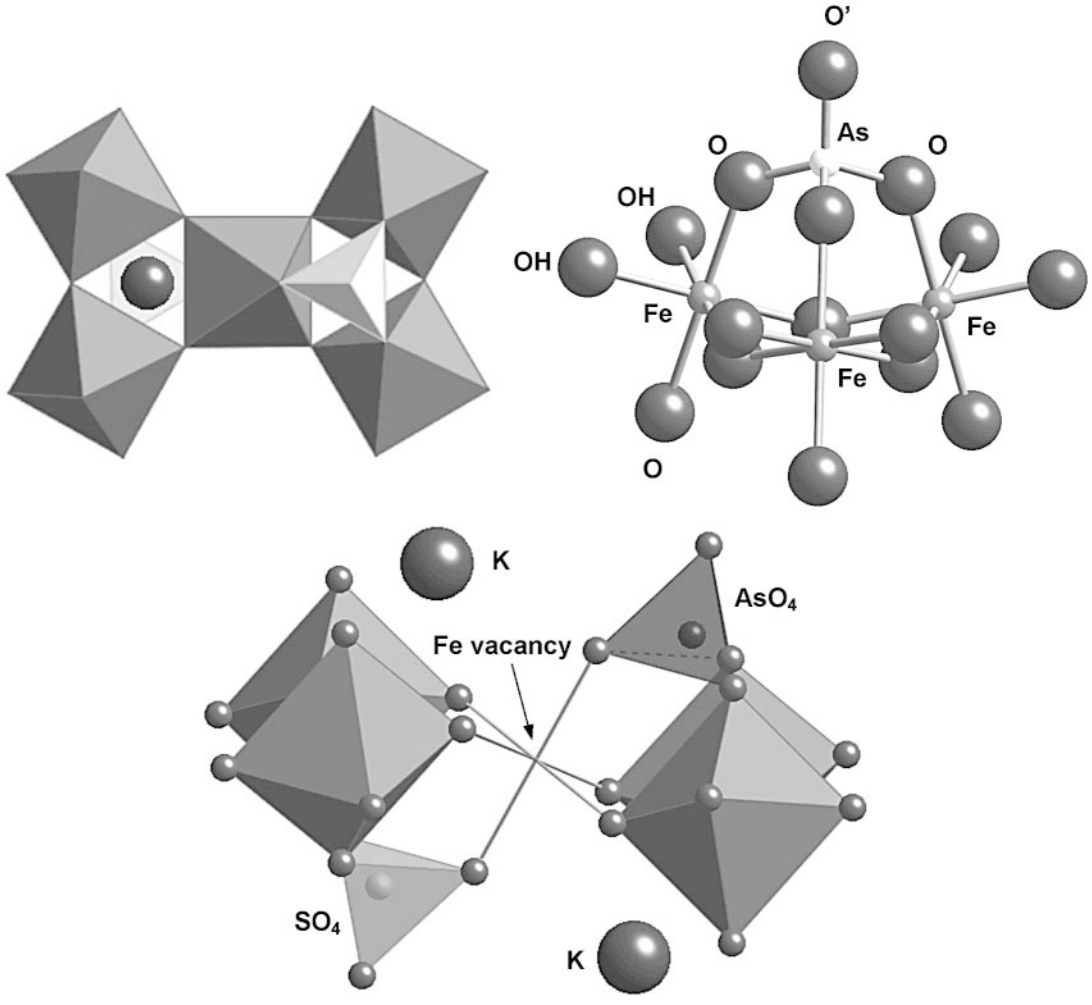

FIG. 8. Local coordination environment around the central As, showing the positions of the O and OH ions and the linkage of the sulfate tetrahedron to the corner-linked Fe–O(OH) octahedra, along with the postulated vacancy in an octahedral site.

Charge-balance considerations

It has long been recognized that both natural and synthetic jarosite-type compounds have stoichiometric deficiencies of "alkali" and iron (Kubisz 1964, Dutrizac & Kaiman 1976). These deficiencies in cation-site occupancies result in an apparent excess of negative charge. The deficiency in alkali-site occupancy was traditionally ascribed to compensating hydronium ion (H_3O^+) substitution, but the presence of hydronium ion is difficult to prove in jarosite-type compounds, which contain OH, SO_4 and small quantities of H_2O. Nevertheless, Ripmeester *et al.* (1986) used NMR techniques with fully deuterated jarosite-type compounds to confirm the postulated presence of hydronium ion and to show that the hydronium content increases, at least semiquantitatively, as the extent of alkali deficiency increases. The deficiency in iron-site occupancy was traditionally rationalized by assuming that some of the OH ions in the Fe–O(OH) octahedra are protonated to H_2O to give Fe–O(OH)(H_2O) octahedra. Presumably, the proton jumps rapidly from OH to OH throughout the structure, as X-ray-diffraction analysis indicates only a single Fe-(OH,H_2O) bond length. Another possible consideration is the protonation of the SO_4^{2-} ions to form the species HSO_4^-, where again the proton would jump rapidly from SO_4 to SO_4 such that only a single S–(O,OH) bond length is detected. Under the acid conditions required for jarosite formation, approximately equal concentrations of SO_4^{2-} and HSO_4^- are present in solution (Pourbaix 1974). Hence, the partial incorporation of bisulfate in jarosite precipitates seems possible, and this mechanism, along with the protonation of some of the OH groups, could maintain the charge balance in arsenic-free jarosite.

The partial incorporation of arsenate ions in the jarosite structure, whereby trivalent AsO_4 groups replace divalent SO_4 groups, accentuates the apparent excess negative charge. For the samples studied, the charge imbalances range from –1.0 for the lowest extent of AsO_4 substitution to –1.3 for the precipitate with 9.91 wt.% AsO_4. The excess negative charges are reduced to –0.9 to –1.2, if the deficient K^+ sites are filled by H_3O^+ (Ripmeester *et al.* 1986). As mentioned above, Fe deficiencies, as high as 17%, are common in synthetic jarosite-type phases, although uncertainties arising from the chemical analyses and the assignment of "water" in the structure always make the charge balances somewhat uncertain. Assuming that the charge imbalance caused by iron deficiencies is compensated by partial protonation of the OH and SO_4 species (see above), then the charge imbalance caused by the presence of 9.9 wt.% AsO_4 becomes –0.3. We postulate that the single or double protonation of the AsO_4^{3-} ion to give $HAsO_4^{2-}$ or $H_2AsO_4^-$ maintains the required balance of charges in the structure; such protonated ions would be consistent with the arsenic species present in the synthesis solutions (Pourbaix 1974). On the basis of the bond-valence concept, the base strength of the apical oxygen is 0.75 v.u. (valence unit), whereas it is 0.67 for the unconfined basal oxygen from the Fe vacancy. The other basal oxygen atoms (2) of the arsenate coordinated to As, Fe and K have base strengths of 0.17 v.u. Thus, the unconfined oxygen as well as the apical oxygen would tend to protonate toward a more stable structure by reducing the base strengths and may actually form $H_2AsO_4^-$ instead of $HAsO_4^{2-}$.

Conclusions

X-ray powder-diffraction analyses indicate that synthetic jarosite is the only phase in six of the seven precipitates studied, thereby limiting the maximum amount of AsO_4 that can be accommodated in the structure to somewhere between 9.9 and 14.8 wt.%, a concentration at which scorodite is detected. The corresponding maximum AsO_4 mole fraction in the tetrahedral sites is 0.17. Increased arsenate substitution in the structure causes the *d* values to increase gradually and results in enlarged unit-cell parameters.

The XANES spectra of the precipitates indicate that As occurs exclusively as As^{5+}, consistent with the valence state of the arsenic in the reagents used for the syntheses.

The EXAFS spectra indicate that the As–O interatomic distances are uniform at 1.68 Å, and the coordination numbers vary from 4.6 ± 1.7 to 5.4 ± 1.7, confirming the tetrahedral coordination of oxygen atoms around As. The As–Fe interatomic distances are 3.25 and 3.26 Å, with the corresponding coordination numbers in the range 1.4 to 2.2. These values would seem to confirm arsenate substitution for sulfate in the structure. The larger arsenic ions in the tetrahedral sites lead to distorted tetrahedra, which are associated with adjacent vacancies at the octahedral sites. Arsenate substitution is limited to approximately 17 mole % or one arsenate group in a unit cell. The iron-site occupancy seems to play some role in determining the extent of arsenate-for-sulfate substitution. There does not appear to be an insurmountable charge-balance difficulty in the substitution of small amounts of arsenate for sulfate, provided that the trivalent AsO_4^{3-} ions are protonated to give the divalent $HAsO_4^{2-}$ or monovalent $H_2AsO_4^-$ species.

Acknowledgements

The XAFS work was carried out at the Stanford Synchrotron Radiation Laboratory, a national user facility operated by Stanford University on behalf of the U.S. Department of Energy, Office of Basic Energy Sciences. Dr. Andrea Foster's help with the XAFS data collection at the Stanford Synchrotron Radiation Laboratory and with data analysis is acknowledged and greatly appreciated. X-ray powder-diffraction analyses were performed by Dr. John Wilson of CANMET. We

thank the referees, Drs. John L. Jambor and Kaye Savage, and Robert F. Martin for their constructive comments on the manuscript.

REFERENCES

ALPERS, C.N., NORDSTROM, D.K. & BALL, J.W. (1989): Solubility of jarosite solid solutions precipitated from acid mine waters, Iron Mountain, California, U.S.A. *Sciences Géologiques Bull.* **42**, 281-298.

BARON, D. & PALMER, C.D. (2002): Solid-solution aqueous-solution reactions between jarosite ($KFe_3(SO_4)_2(OH)_6$) and its chromate analog. *Geochim. Cosmochim. Acta* **66**, 2841-2853.

BAUR, W.H. (1981): Interatomic distance predictions for computer simulation of crystal structures. *In* Structure and Bonding in Crystals **2** (M. O'Keeffe & A. Navrotsky, eds.). Academic Press, New York, N.Y. (31-52).

BROPHY, G.P. & SHERIDAN, M.F. (1965): Sulfate studies. IV. The jarosite – natrojarosite – hydronium jarosite solid solution series. *Am. Mineral.* **50**, 1595-1607.

DUTRIZAC, J.E. (1983): Factors affecting alkali jarosite formation. *Metall. Trans.* **14B**, 531-539.

_____, DINARDO, O. & KAIMAN, S. (1981): Selenate analogues of jarosite-type compounds. *Hydrometall.* **6**, 327-337.

_____ & JAMBOR, J.L. (1984): Formation and characterization of argentojarosite and plumbojarosite and their relevance to metallurgical processing. *In* Proc. Second Int. Congress on Applied Mineralogy in the Minerals Industry (W.C. Park, D.M. Hausen & R.D. Hagni, eds.). AIME, New York, N.Y. (507-530).

_____ & _____ (1987): The behaviour of arsenic during jarosite precipitation: arsenic precipitation at 97°C from sulphate or chloride media. *Can. Metall. Quart.* **26**, 91-101.

_____ & _____ (2000): Jarosites and their application in hydrometallurgy. *In* Sulfate Minerals: Crystallography, Geochemistry, and Environmental Significance (C.N. Alpers, J.L. Jambor & D.K. Nordstrom, eds.). *Rev. Mineral. Geochem.* **40**, 405-452.

_____, _____ & CHEN, T.T. (1987): The behaviour of arsenic during jarosite precipitation: reactions at 150°C and the mechanism of arsenic precipitation. *Can. Metall. Quart.* **26**, 103-115.

_____ & KAIMAN, S. (1976): Synthesis and properties of jarosite-type compounds. *Can. Mineral.* **14**, 151-158.

FENDORF, S., EICK, M.J., GROSSL, P. & SPARKS, D. (1997): Arsenate and chromate retention mechanisms on goethite. 1. Surface structure. *Environ. Sci. Technol.* **31**, 315-320.

FOSTER, A.L. (1999): *Partitioning and Transformation of Arsenic and Selenium in Natural and Laboratory Systems*. Ph.D. thesis, Stanford Univ., Stanford, California.

_____, BROWN, G.E., JR. TINGLE, T.N. & PARKS, G.A. (1998): Quantitative arsenic speciation in mine tailings using X-ray absorption spectroscopy. *Am. Mineral.* **83**, 553-568.

GEORGE, G.N. & PICKERING, I.J. (1993): *EXAFSPAK: a Suite of Computer Programs for Analysis of X-ray Absorption Spectra*. Stanford Synchrotron Radiation Laboratory, Palo Alto, California.

HAWTHORNE, F.C., KRIVOVICHEV, S.V. & BURNS, P.C. (2000): The crystal chemistry of sulfate minerals. *In* Sulfate Minerals: Crystallography, Geochemistry, and Environmental Significance (C.N. Alpers, J.L. Jambor & D.K. Nordstrom, eds.). *Rev. Mineral. Geochem.* **40**, 1-112.

HAYES, K.F., ROE, A.L., BROWN, G.E., HODGSON, K.O., LECKIE, J.O. & PARKS, G.A. (1987): In situ X-ray absorption study of surface complexes: selenium oxyanions on α-FeOOH. *Science* **238**, 783-786.

KATO, T. & MIÚRA, Y. (1977): The crystal structure of jarosite and svanbergite. *Mineral. J.* **8**, 419-430.

KOLITSCH, U. & PRING, A. (2001): Crystal chemistry of the crandallite, beudantite and alunite groups: a review and evaluation of the suitability as storage materials for toxic metals. *J. Mineral. Petrol. Sci.* **96**, 67-78.

KRAUSE, E. & ETTEL, V.A. (1989): Solubilities and stabilities of ferric arsenate compounds. *Hydrometall.* **22**, 311-337.

KUBISZ, J. (1964): A study on minerals of the alunite–jarosite group. *Polska Akad. Nauk, Prace Geol.* **22**, 1-93.

MENCHETTI, S. & SABELLI, C. (1976): Crystal chemistry of the alunite series: crystal structure refinement of alunite and synthetic jarosite. *Neues Jahrb. Mineral., Monatsh.*, 406-417.

PAKTUNC, A.D. (1998): MODAN: an interactive computer program for estimating mineral quantities based on bulk composition. *Comput. Geosci.* **24**, 425-431.

_____, FOSTER, A., HEALD, S. & LAFLAMME, G. (2003a): Speciation and characterization of arsenic in gold ores and cyanidation tailings using X-ray absorption spectroscopy. *Geochim. Cosmochim. Acta* (in press).

_____, _____, & LAFLAMME, G. (2003b): Speciation and characterization of arsenic in Ketza River mine tailings using X-ray absorption spectroscopy. *Environ. Sci. Technol.* **37**, 2067-2074.

PAULING, L. (1929): The principles determining the structure of complex ionic crystals. *J. Am. Chem. Soc.* **51**, 1010-1026.

PETERSON, M.L., BROWN, G.E., PARKS, G.A. & STEIN, C.L. (1997): Differential redox and sorption of Cr(III/VI) on natural silicate and oxide minerals: EXAFS and XANES results. *Geochim. Cosmochim. Acta* **61**, 3399-3412.

POURBAIX, M. (1974): *Atlas of Electrochemical Equilibria*. National Association of Corrosion Engineers, Houston, Texas.

RANDALL, S.R., SHERMAN, D.M. & RAGNARSDOTTIR, K.V. (2001): Sorption of As(V) on green rust ($Fe_4(II)Fe_2(III)(OH)_{12}SO_4 \cdot 3H_2O$) and lepidocrocite (α-FeOOH): surface complexes from EXAFS spectroscopy. *Geochim. Cosmochim. Acta* **65**, 1015-1023.

RIPMEESTER, J.A., RATCLIFFE, C.I., DUTRIZAC, J.E. & JAMBOR, J.L. (1986): Hydronium ion in the alunite–jarosite group. *Can. Mineral*. **24**, 435-447.

ROCA, A., VIÑALS, J., ARRANZ, M. & CALERO, J. (1999): Characterization and alkaline decomposition/cyanidation of beudantite-jarosite materials from Rio Tinto gossan ores. *Can. Metall. Quart.* **38**, 93-103.

SAVAGE, K.S., BIRD, D.K & O'DAY, P.A. (2003): Arsenic speciation in synthetic jarosite. *Chem. Geol.* (in press).

_____, TINGLE, T.N., O'DAY, P.A., WAYCHUNAS, G.A. & BIRD, D.K. (2000): Arsenic speciation in pyrite and secondary weathering phases, Mother Lode gold district, Tuolumne County, California. *Appl. Geochem.* **15**, 1219-1244.

SHANNON, R.D. (1976): Revised effective ionic radii and systematic studies of interatomic distances in halides and chalcogenides. *Acta Crystallogr.* **A32**, 751-767.

STOILOVA, D., WILDNER, M. & KOLEVA, V. (2003): Vibrational behaviour of the S–O stretches in compounds with kröhnkite-type chains $Na_2Me(SeO_4)_2 \cdot 2H_2O$ with matrix-isolated SO_4^{2-} and Me^{2+} guest ions (Me = Mn, Co, Ni, Cu, Zn, Cd). *Vibrational Spectros.* **31**, 115-123.

SZYMAŃSKI, J.T. (1988): The crystal structure of beudantite, $Pb(Fe,Al)_3[(As,S)O_4]_2(OH)_6$. *Can. Mineral.* **26**, 923-932.

WAYCHUNAS, G.A., REA, B.A., FULLER, C.C. & DAVIS, J.A. (1993): Surface chemistry of ferrihydrite. 1. EXAFS studies of the geometry of coprecipitated and adsorbed arsenate. *Geochim. Cosmochim. Acta* **57**, 2251-2269.

_____, XU, N., FULLER, C.C., DAVIS, J.A. & BIGHAM, J.M. (1995): XAS study of AsO_4^{3-} and SeO_4^{2-} substituted schwertmannites. *Physica B* **208–209**, 481-483.

ZABINSKY, S.I., REHR, J.J., ANKUDINOV, A., ALBERS, R.C. & ELLER, M.J. (1995): Multiple-scattering calculation of x-ray-absorption spectra. *Phys. Rev.* B **52**, 2995-3009.

Received January 27, 2003, revised manuscript accepted July 16, 2003.